

Synthesis and theoretical design of the novel compound 6,6'-(1,3,4-oxadiazole-2,5-diyl)bis(3-chloroaniline): Reactivity, molecular docking and corrosion inhibition

Assiya Atif^{a*}, Soukaina Ameur^{a,b} and Houssine Ait Sir^a

^aBioorganic Chemistry Team, Laboratory of Bioorganic Chemistry, Faculty of Sciences, Chouaib Doukkali University, 24000 El Jadida, Morocco

^bMolecular Modeling and Spectroscopy Research Team, Faculty of Sciences, Chouaib Doukkali University, 24000 El Jadida, Morocco

CHRONICLE

Article history:

Received June 25, 2025

Received in revised form

July 28, 2025

Accepted January 27, 2026

Available online

January 27, 2026

Keywords:

Synthesis

Characterization

1,3,4-oxadiazole

DFT

Reactivity

ADMET

Molecular Docking

Monte Carlo

Molecular Dynamics

Corrosion inhibitor

ABSTRACT

This study presents the synthesis and characterization of the novel compound 6,6'-(1,3,4-oxadiazole-2,5-diyl)bis(3-chloroaniline), using ¹H NMR, ¹³C NMR, mass spectrometry and FTIR-ATR infrared spectroscopy. Density Functional Theory (DFT) calculations at the B3LYP/6-311G (d,p) level, were employed to optimize the molecular geometry and evaluate electronic properties. Frontier molecular orbital, molecular electrostatic potential, Parr function, and electron localization function analyses revealed an ambiphilic character, with electrophilic sites localized on the oxadiazole core and nucleophilic regions on the chloroaniline moieties. Molecular docking demonstrated high binding affinities toward Topoisomerase IV, Tubulin, and CDK2, surpassing standard ligands and indicating potential antibacterial and anticancer activities. ADME/Toxicity predictions suggested good pharmacokinetic behavior and low toxicity. Monte Carlo and molecular dynamics simulations confirmed strong and stable adsorption of the novel compound OBA on the Fe (110) surface, supporting its efficiency as a corrosion inhibitor.

1. Introduction

In medicinal chemistry, heterocyclic structures are among the most analyzed due to their importance in drug development¹. These compounds are essential building blocks for many bioactive molecules, contributing to their therapeutic properties². Oxadiazole is one of these heterocyclic systems: a five-membered ring structure incorporating one oxygen atom, two nitrogen atoms, and two double bonds³ maceutical research⁴. In recent years, many detailed studies have been carried out on oxadiazole derivatives, highlighting their therapeutic potential for various diseases and pharmacological conditions⁵.

Several vital structures, such as pyrrole, oxadiazole, thiadiazole, and triazole⁶⁻⁸, have gained importance due to their biological relevance among five-membered heterocyclic systems⁹. These heterocyclic structures are found in many bioactive compounds, improving their therapeutic properties¹⁰. 1,3,4-Oxadiazole is of particular interest to scientists due to its diverse pharmacological activities¹¹. The presence of the oxadiazole nucleus in several therapeutic candidates has been linked to increased biological efficacy, positioning it as a crucial component of pharmaceutical chemistry¹².

Scientific research has demonstrated the wide range of biological activities of 1,3,4-oxadiazole derivatives¹³. These substances have proven to have potent antimicrobial properties, making them useful in combating various bacterial and mycological infections¹⁴. Furthermore, their antituberculous action suggests potential applications in the treatment of

* Corresponding author

E-mail address assia.atif@gmail.com (A. Atif)

© 2026 by the authors; licensee Growing Science, Canada

doi: 10.5267/j.ccl.2026.1.006

tuberculosis¹⁵. These molecules, thanks to their vascular dilating effects that are beneficial in cardiovascular treatments, while possessing cytotoxic and antitumor properties, show promise in the fight against cancer¹⁶. In addition, 1,3,4-oxadiazole compounds possess painkilling and anti-inflammatory properties that make them useful for the treatment of pain and inflammatory diseases¹⁷. Additional pharmacological activities, such as hypolipidemic and ulcerogenic properties, further extend their therapeutic potential¹⁸.

Thanks to their multiple biological properties and structural flexibility, 1,3,4-oxadiazole compounds remain at the center of current research for the discovery of new drugs¹⁹. Their ability to interact with different biological targets positions them as attractive candidates for the development of new treatments²⁰. These compounds therefore offer considerable potential for the pharmaceutical sector, paving the way for the identification of new effective remedies for a variety of diseases²¹.

In this context, the novel compound 6,6'-(1,3,4-Oxadiazole-2,5-diyl)bis(3-chloroaniline) noted as OBA was selected as a model molecule for theoretical investigation. To gain deeper insight into its electronic behavior, chemical reactivity, and biological potential, a comprehensive *in silico* study was carried out. Quantum chemical calculations based on Density Functional Theory (DFT) were employed to examine the molecular stability, charge distribution, and reactive sites through the analysis of the frontier molecular orbitals (HOMO and LUMO), Molecular Electrostatic Potential (MEP), Parr function, and Electron Localization Function (ELF). These electronic descriptors provide valuable information on the donor-acceptor interactions and adsorption capability of the novel compound OBA, which are crucial in understanding its corrosion inhibition efficiency on metallic surfaces. In parallel, molecular docking simulations were performed to predict and compare the binding affinities of the novel compound OBA with selected protein targets related to antibacterial and anticancer activities. The combined quantum chemical and docking approaches provide a complementary view of the compound's reactivity, interaction potential, and multifunctional applications.

2. Materials and Methods

2.1 Reagents and instruments

All reagents and solvents were obtained from Sigma Aldrich and used as received. Reaction progress is monitored by thin-layer chromatography (TLC) on aluminum sheets coated with Merck 60 F254 silica gel (thickness 0.2 nm). Revelation is carried out under a UV-Visible lamp (at 254 and 365 nm). The melting points of the synthesized compounds were determined using a Köfler bench and to degrees Celsius. FTIR spectra were recorded on a SHIMADZU FT-IR 8400S spectrometer with a Smart iTR accessory and attenuated with total reflection crystal diamond (ATR) in the range (500-4000 cm^{-1}). The spectra were recorded on a JNM-ECZ500/S1 FT NMR SYSTEM (JEOL) Fourier transform spectrometer (500 MHz for the proton and 125 MHz for carbon-13) at the National Center for Scientific and Technical Research (CNRST) in Rabat. The spectra are referenced to the DMSO solvent at room temperature. High-resolution mass spectrometry (HRMS) was performed using an Ultimate 3000-Exactive Plus Thermo quadrupole-Orbitrap mass spectrometer, equipped with a collision cell, also housed at the CNRST in Rabat.

2.2 Calculation methodology

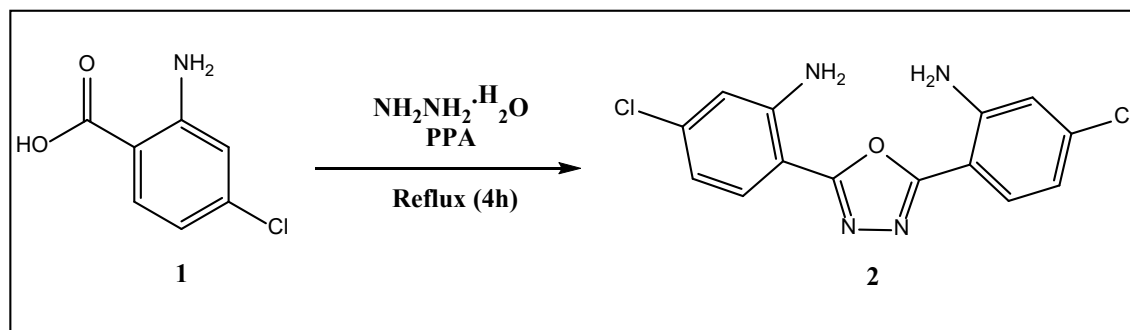
The reactivity, corrosion inhibition potential, and biological interactions of the novel compound 6,6'-(1,3,4-Oxadiazole-2,5-diyl)bis(3-chloroaniline) (OBA) were investigated using a combination of quantum chemical calculations²²⁻²⁷, molecular docking²⁸, and ADME/Toxicity predictions. Molecular structures were drawn in ChemDraw and optimized using Density Functional Theory (DFT) at the B3LYP/6-311G(d,p) level, performed with Gaussian 09 and visualized with GaussView 6, a method and basis set validated for heterocyclic compounds, providing accurate electronic properties with moderate computational cost²⁹⁻³⁰. Reactivity descriptors, including frontier molecular orbitals (HOMO and LUMO), Molecular Electrostatic Potential (MEP) surfaces, and the Parr function, were analyzed to identify reactive sites, while the Electron Localization Function (ELF) was calculated to examine electron density and bonding patterns³¹. Molecular visualization was performed using VMD³². Corrosion inhibition potential was evaluated using calculated electronic parameters and adsorption descriptors. ADME and toxicity profiles were predicted using the PKCSM web tool³³. Molecular docking simulations were conducted with AutoDock Vina³⁴ against protein targets associated with anticancer and antibacterial activities. Protein structures were obtained from the Protein Data Bank (PDB)³⁵, and reference ligands from PubChem³⁶ were used for comparison. Docking results were visualized using Maestro (Schrödinger).

2.3 Synthesis of the novel compound 6,6'-(1,3,4-Oxadiazole-2,5-diyl)bis(3-chloroaniline) (2)

The novel compound 6,6'-(1,3,4-Oxadiazole-2,5-diyl)bis(3-chloroaniline) (**2**) was synthesized by reacting two equivalents of 2-amino-4-chlorobenzoic acid (**1**) with one equivalent of hydrazine hydrate in polyphosphoric acid (5 ml) at reflux for 4 hours. At the end of the reaction, the mixture was neutralized with sodium hydroxide NaOH to pH = 7. The solid formed was filtered, washed and recrystallized from ethanol³⁷. **Appearance:** Solid Beige, **yield:** 95%, **m.p:** 206°C, **¹H NMR(500MHz/DMSO-*d*₆,ppm):** 6.59(s,4H,NH₂), 7.16(s,2H,CHar), 7.59(d,J=5 Hz,2H,CHar), 7.93(d,J=5 Hz,2H,CHar), **¹³C NMR (125MHz/DMSO-*d*₆, ppm) :** 162.86(2C=N), 146.80(2Car), 135.52(2Car), 128.79(2Car), 121.62(2Car), 117.66(2Car), 115.51(2Car), **IR (cm⁻¹):** 3321-3448 ν NH₂, 1614 ν C=N, **MS(ESI):** m/z = 321 [M+H]⁺

3. Results and Discussion

Various methods have been cited in the literature for the synthesis of 1,3,4-oxadiazole derivatives³⁸⁻⁴¹. In this work, two equivalents of 2-amino-4-chlorobenzoic acid (**1**) were reacted with hydrazine hydrate in the presence of polyphosphoric acid at reflux for 4 hours to obtain the novel compound 6,6'-(1,3,4-Oxadiazole-2,5-diyl)bis(3-chloroaniline) (**2**)³⁷



Scheme 1. Synthesis of the novel compound 6,6'-(1,3,4-Oxadiazole-2,5-diyl)bis(3-chloroaniline)

The analysis of the ¹H NMR spectrum of the novel compound 6,6'-(1,3,4-Oxadiazole-2,5-diyl)bis(3-chloroaniline), highlights a singlet at 6.59 ppm integrating four protons of the amine group and clusters between 7.16 and 7.93 ppm corresponding to the aromatic protons. The ¹³C NMR spectrum shows a signal at 162.86 ppm attributable to the C=N bond and signals at 146.80, 135.52, 128.79, 121.62, 117.66 and 115.51 ppm due to the aromatic carbons. The spectrum highlights two bands at 3321-3448 cm⁻¹ relating to N-H of the amine and a band at 1614 cm⁻¹ corresponding to the C=N bond. The mass spectrum, taken in (ESI), shows a molecular peak related to the molecular ion m/z = 321[M+H]⁺.

3.1 Analysis of the Electronic Structure of the novel compound 6,6'-(1,3,4-Oxadiazole-2,5-diyl)bis(3-chloroaniline)

We examined the electronic structure and reactivity descriptors of the novel compound 6,6'-(1,3,4-oxadiazole-2,5-diyl)bis(3-chloroaniline). Based on the Electron Localization Function (ELF) analysis, Lewis-like representations were constructed to illustrate the main localization domains and corresponding valence basin populations. The resulting ELF topologies and electronic density distributions are presented in **Fig. 1**.

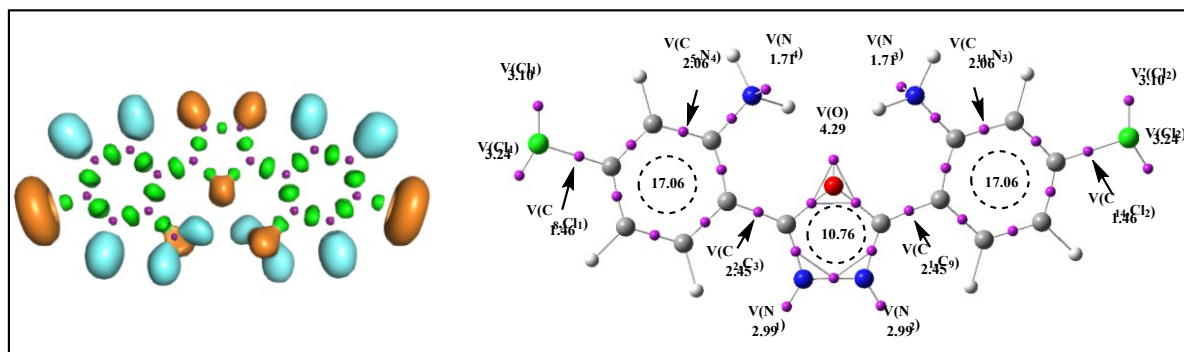


Fig. 1. ELF localization domains and basin attractor positions together with the most significant valence basin populations of the novel compound 6,6'-(1,3,4-oxadiazole-2,5-diyl)bis(3-chloroaniline)

Electron Localization Function (ELF) analysis of the novel compound 6,6'-(1,3,4-oxadiazole-2,5-diyl)bis(3-chloroaniline) reveals both monosynaptic and disynaptic basins, reflecting electron localization in bonds and lone pairs. The central oxadiazole ring exhibits a total delocalized electron density of 10.76e, with highly localized O and N lone pairs (4.29e and 2.99e, respectively) indicating strong nucleophilicity. Disynaptic C–N and C–C bonds in the ring show typical electron sharing (2.45e). In the 3-chloroaniline groups, aromatic C–C and C–N bonds display standard delocalization, while amine N lone pairs (1.71e) and polarized C–Cl bonds (1.46e) suggest electrophilic and nucleophilic sites, respectively. The aromatic rings contribute 17.06e in delocalized π -electron density, supporting resonance stabilization and potential π – π interactions, relevant for molecular docking studies.

Table 1: HOMO, LUMO, electronic chemical potential (μ), chemical hardness (η), electrophilicity index (ω), and nucleophilicity index (N) of the novel compound 6,6'-(1,3,4-oxadiazole-2,5-diyl)bis(3-chloroaniline) (OBA), expressed in (eV).

Compound	HOMO	LUMO	N	ω	μ	η
OBA	-6.04	-1.95	3.33	3.90	-4.00	2.05

The frontier molecular orbitals (FMOs) of the novel compound OBA were analyzed to assess its chemical and electronic reactivity. The HOMO and LUMO energies are calculated as -6.04 eV and -1.95 eV, respectively, corresponding to a HOMO-LUMO gap of 4.09 eV (**Fig. 2**). This moderate gap indicates that the novel compound OBA possesses considerable chemical stability while maintaining sufficient reactivity for potential electron transfer interactions. From a chemical perspective, this balance between stability and reactivity put forward that the novel compound OBA might participate efficiently in experimentally observed reactions without experiencing rapid degradation, making it a fit candidate for further functionalization and biological evaluation. Furthermore, the gap suggests that electronic excitation would require photons of energy approximately 4.09 eV, which corresponds to the ultraviolet (UV) region. Therefore, OBA could potentially absorb UV light, making it relevant for photochemical or photoinduced processes.

The global nucleophilicity index N , evaluated relative to tetracyanoethylene (TCE) as a reference, is 3.33 eV, indicating that the novel compound OBA is a strong nucleophile, with a significant ability to donate electrons to electrophilic centers. Simultaneously, the electrophilicity index $\omega=3.90$ eV suggests that the molecule can also act as an electrophile, highlighting its ambiphilic character. The chemical potential $\mu=-4.00$ eV indicates a tendency to retain electron density, while the chemical hardness $\eta=2.05$ eV reflects a balanced reactivity profile, allowing moderate deformation of the electron cloud during interactions (**Table 1**). These global reactivity descriptors specify that the novel compound OBA can engage in both electron-donating and electron-accepting interactions, which is reliable with its potential contribution in charge-transfer processes observed experimentally. Such ambiphilic behavior is particularly beneficial in molecular docking, where simultaneous nucleophilic and electrophilic interactions with amino acid residues can improve binding affinity.

Analysis of the spatial distribution of the HOMO and LUMO orbitals reveals that the HOMO is primarily localized over the electron-rich 3-chloroaniline moieties, identifying these sites as the most reactive centers for nucleophilic attack, whereas the LUMO is mainly distributed over the 1,3,4-oxadiazole core, suggesting it is the preferred site for electrophilic interactions. This distribution aligns with the global reactivity indices and supports the ambiphilic behavior of the novel compound OBA. From a reactivity standpoint, the localization of the HOMO on the 3-chloroaniline moieties suggests that these regions are likely involved in experimentally appropriate nucleophilic interactions, while the LUMO localization on the oxadiazole ring highlights this fragment as a key acceptor site through electrophilic attack. In the context of molecular docking, this electronic distribution explains the preferential interactions of the oxadiazole core with electron-rich residues and the aniline moieties with electrophilic or hydrogen-bond-accepting sites in the protein active site.

The HOMO-LUMO gap further implies that the novel compound OBA may exhibit photoresponsive behavior, as the gap corresponds to an energy absorption in the UV range. Such properties are relevant for applications in photochemistry, UV-induced cycloadditions, and molecular docking studies involving photoactive targets, where excitation can modulate electron density and reactivity. Consequently, the photo-responsive nature inferred from the HOMO-LUMO gap may promote influence the reactivity and binding behavior of OBA under irradiation, posing potential advantages in photoactivated biological or catalytic applications.

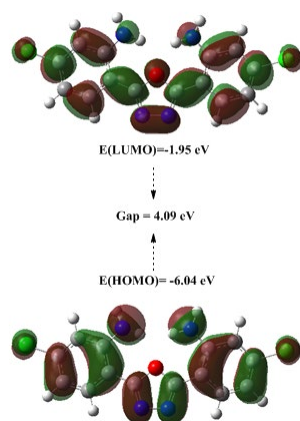


Fig. 2. HOMO and LUMO energy levels of the novel compound OBA along with the calculated HOMO–LUMO energy gap ($\Delta E = 4.09$ eV)

3.2 Parr function analysis and Molecular Electrostatic Potential (MEP)

Parr functions and Molecular Electrostatic Potential (MEP) are complementary computational tools for analyzing molecular reactivity. Parr functions identify electrophilic and nucleophilic sites based on electron density, with positive values indicating nucleophilic centers and negative values indicating electrophilic centers. MEP maps visualize the electrostatic charge distribution, highlighting electron-rich (negative potential) and electron-deficient (positive potential) regions. Together, they provide a clear picture of reactive sites, guiding predictions of chemical interactions, hydrogen bonding, and docking behavior. (**Fig 3**)

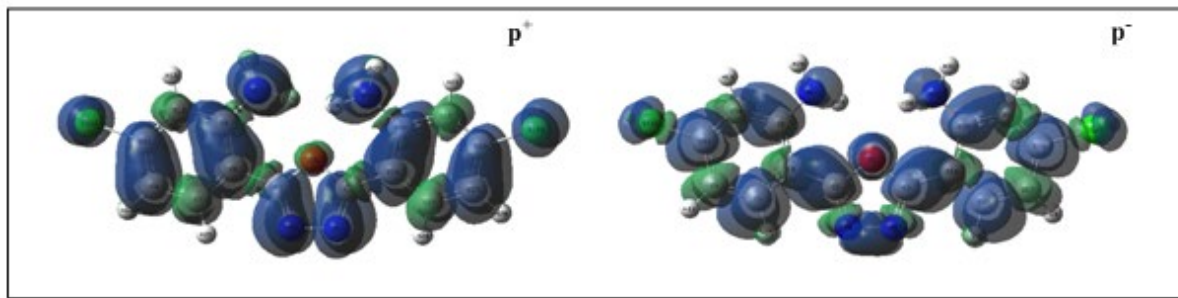
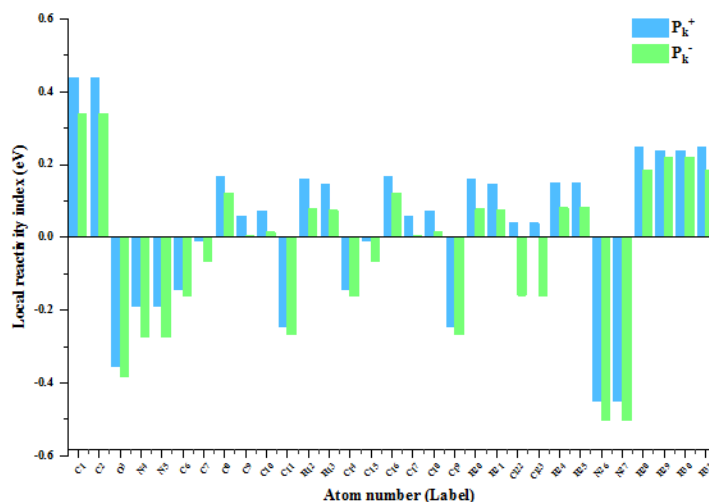


Fig. 3. 3D Mulliken spin densities of the novel compound 6,6'-(1,3,4-oxadiazole-2,5-diyl)bis(3-chloroaniline) (OBA).



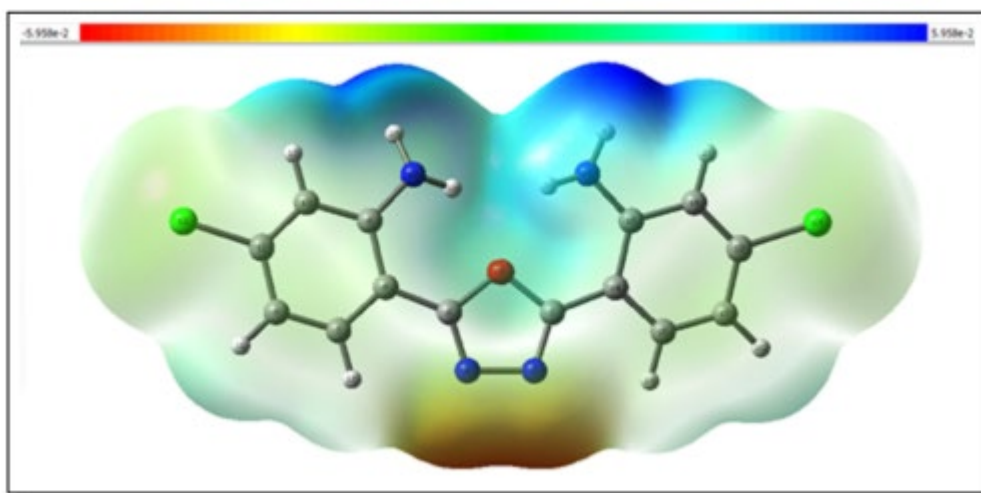


Fig. 5. 3D molecular electrostatic potential (MEP) map of the novel compound 6,6'-(1,3,4-oxadiazole-2,5-diyl)bis(3-chloroaniline) (OBA).

The 3D molecular electrostatic potential (MEP) map of the novel compound 6,6'-(1,3,4-oxadiazole-2,5-diyl)bis(3-chloroaniline) (**Fig. 5**) reveals regions of varying electron density corresponding to nucleophilic and electrophilic sites. The central oxadiazole ring exhibits electron-rich regions (light red/orange), indicating a propensity for nucleophilic attacks; these electron-rich areas are likely to preferentially interact with electrophilic species in chemical reactions, providing a rational clarification for experimentally observed regioselectivity connecting the oxadiazole core, while the 3-chloroaniline moieties display slightly electron-deficient areas (green to light blue), suggesting potential electrophilic character. Such electron-deficient zones may assist interactions with nucleophilic functional groups or negatively charged residues within biological targets. The chlorine atoms show localized negative potential, consistent with their electronegativity, whereas the NH groups are slightly positive, highlighting sites for hydrogen bonding or electrophilic interactions. Such regions are especially pertinent, as hydrogen-bond donors and acceptors mostly manage ligand attaching and orientation in protein active sites. Therefore, polarized NH groups may contribute substantially to binding stability and specificity.

The novel compound OBA demonstrates ambiphilic behavior, with the oxadiazole core favoring nucleophilic reactivity and the NH/aromatic regions prone to electrophilic interactions, aligning with its global reactivity indices ($N = 3.33$ eV, $\omega = 3.90$ eV).

3.3 Non-Covalent Interaction (NCI) Analysis and Implications for Molecular Docking

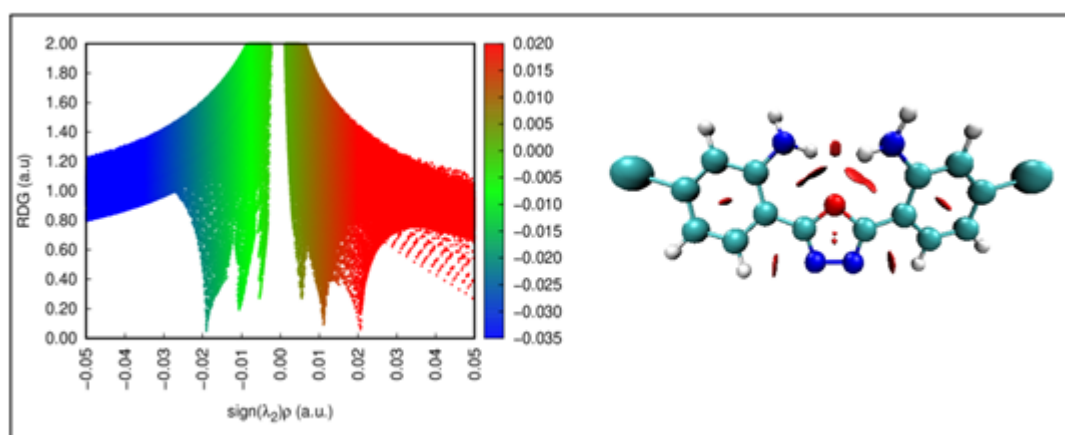


Fig. 6. Non-Covalent Interaction (NCI) analysis of the novel compound 6,6'-(1,3,4-oxadiazole-2,5-diyl)bis(3-chloroaniline) (OBA), visualized using VMD.

The Non-Covalent Interaction (NCI) analysis of the novel compound 6,6'-(1,3,4-oxadiazole-2,5-diyl)bis(3-chloroaniline) (OBA) was performed using VMD to visualize the distribution of stabilizing and repulsive interactions within the molecule. The 3D RDG isosurfaces and the RDG plot reveal distinct regions of interaction: blue regions correspond to strong attractive forces such as hydrogen bonding and electrostatic interactions, green regions indicate weak van der Waals or dispersive contacts, and red regions highlight areas of steric repulsion. This classification permits a direct assessment of the nature and strength of intramolecular interactions that manage molecular stability and recognition behavior. In the novel compound OBA, significant green and blue zones are observed around the oxadiazole ring and near the $-NH$ and $-Cl$

substituents, suggesting that both dispersive forces and localized electrostatic attractions contribute to molecular stability. Such stabilizing non-covalent interactions are usually involved in experimentally observed ligand–receptor recognition processes. In particular, hydrogen bonding and dispersive contacts are known to show a decisive role in modulating binding affinity and selectivity in biological systems. The limited presence of red regions indicates minimal steric hindrance, confirming that the molecule adopts a favorable conformation for intermolecular binding. This favorable steric profile suggests that the novel compound OBA can freely adapt to confined environments such as protein binding pockets without significant conformational strain, which is beneficial for stable ligand-protein complex formation. Importantly, the identified van der Waals and hydrogen-bonding regions define potential interaction sites that can act as hotspots in molecular docking studies, guiding the selection of protein residues for optimal binding. These non-covalent features provide insight into the likely orientation and affinity of the novel compound OBA when interacting with biological targets, supporting rational docking predictions and ligand design (**Fig. 6**).

3.4 ADME and Toxicological Evaluation

The pharmacokinetic and toxicity profiles of the novel compound 6,6'-(1,3,4-oxadiazole-2,5-diyl)bis(3-chloroaniline) (OBA) were evaluated using *in silico* predictions. ADME (Absorption, Distribution, Metabolism, and Excretion) properties provide insights into the compound's bioavailability, solubility, permeability, and metabolic interactions, while toxicity predictions help assess safety for further biological or industrial applications. Understanding these properties is crucial before performing molecular docking studies and exploring potential applications.

Table 2. *In silico* predicted absorption, distribution, metabolism, and excretion (ADME) properties of the novel compound 6,6'-(1,3,4-oxadiazole-2,5-diyl)bis(3-chloroaniline).

Property	Model Name	Predicted Value
Absorption	Water solubility	-3.624 (log mol/L)
	Caco2 permeability	0.967 (log Papp in 10 ⁻⁶ cm/s)
	Intestinal absorption (human)	89.423 (% Absorbed)
	Skin Permeability	-2.77 (log Kp)
	P-glycoprotein substrate	Yes
	P-glycoprotein I inhibitor	No
	P-glycoprotein II inhibitor	Yes
Distribution	VDss (human)	0.097 (log L/kg)
	Fraction unbound (human)	0.112 (Fu)
	BBB permeability	-0.708 (log BB)
Metabolism	CNS permeability	-1.909 (log PS)
	CYP2D6 substrate	No
	CYP3A4 substrate	Yes
	CYP1A2 inhibitor	Yes
	CYP2C19 inhibitor	Yes
	CYP2C9 inhibitor	Yes
	CYP2D6 inhibitor	No
Excretion	CYP3A4 inhibitor	Yes
	Total Clearance	-0.102 (log ml/min/kg)
	Renal OCT2 substrate	No

The novel compound OBA demonstrates favorable oral absorption, with moderate water solubility (-3.624 log mol/L), high intestinal absorption (89%), and moderate Caco-2 permeability (0.967 log Papp), while skin permeability is low (-2.77 log Kp). It is a P-glycoprotein substrate and selectively inhibits P-gp II, suggesting possible efflux effects on bioavailability. Distribution is limited, as indicated by a low volume of distribution (0.097 log L/kg) and moderate plasma protein binding (Fu = 0.112), with poor BBB (-0.708 log BB) and CNS (-1.909 log PS) penetration. Metabolically, the novel compound OBA is a CYP3A4 substrate and inhibits several CYP isoforms (CYP1A2, CYP2C19, CYP2C9, and CYP3A4), indicating potential drug–drug interactions. Excretion is slow, with low total clearance (-0.102 log mL/min/kg) and no involvement of renal OCT2 transporters. Overall, these properties suggest good oral bioavailability, limited tissue and CNS distribution, metabolic interaction potential, and predominantly non-renal elimination. (**Table 2**)

Table 3. Predicted toxicity profile of the novel compound 6,6'-(1,3,4-oxadiazole-2,5-diyl)bis(3-chloroaniline) (OBA) based on *in silico* models, including mutagenicity, hepatotoxicity, cardiotoxicity, acute and chronic toxicity, skin sensitization, and aquatic toxicity.

Property	Predicted Value (with Unit)
AMES toxicity	No
Max. tolerated dose (human)	0.124 (log mg/kg/day)
hERG I inhibitor	No
hERG II inhibitor	No
Oral Rat Acute Toxicity (LD50)	2.918 (mol/kg)
Oral Rat Chronic Toxicity (LOAEL)	0.919 (log mg/kg_bw/day)
Hepatotoxicity	No
Skin Sensitisation	No
T.Pyriformis toxicity	0.385 (log µg/L)
Minnow toxicity	-0.227 (log mM)

The novel compound OBA exhibits a favorable safety profile, being predicted as non-mutagenic (AMES negative), non-hepatotoxic, non-sensitizing, and lacking inhibition of hERG I and II channels, indicating minimal cardiotoxic risk. Acute ($LD_{50} = 2.918$ mg/kg) and chronic ($LOAEL = 0.919$ log mg/kg_bw/day) toxicity values suggest acceptable safety margins, while low *T. pyriformis* and Minnow toxicity indicate minimal environmental impact. The predicted human maximum tolerated dose (0.124 log mg/kg/day) is moderate, further supporting its relative safety for experimental and pharmacological applications. (Table 3)

Based on its structural features and predicted safety, the novel compound OBA represents a promising candidate for investigation of therapeutic activities, including antibacterial, antifungal, anti-inflammatory, or anticancer potential, depending on the chosen protein targets. Furthermore, given its chemical structure and the established properties of oxadiazole derivatives, the novel compound OBA may serve as an effective corrosion inhibitor by adsorbing onto metal surfaces and preventing oxidation. Docking studies against metals such as Fe or Cu could provide detailed mechanistic insights into these interactions.

3.5 Docking-Based Evaluation of Biological Binding Affinity

To evaluate the potential biological activities of the novel compound 6,6'-(1,3,4-oxadiazole-2,5-diyl)bis(3-chloroaniline) (OBA), molecular docking studies were carried out against selected antibacterial and anticancer targets. Topoisomerase IV (PDB ID: 3FOF) was chosen for its essential role in bacterial DNA replication, with levofloxacin as a reference ligand. For anticancer activity, Tubulin (PDB ID: 1SA0) and Cyclin-Dependent Kinase 2 (CDK2) (PDB ID: 1FIN) were selected, using colchicine and roscovitine as reference ligands, respectively. These proteins are key regulators of cell division and proliferation, making them relevant targets to assess the therapeutic potential of the novel compound OBA. (Table 4)

Table 4. Molecular Docking Comparison of the novel compound OBA and Reference Compounds with Target Proteins

Activity	Target Protein	PDB ID	Ligand	Binding Energy (kcal/mol)
Antibacterial	Topoisomerase IV	3FOF	OBA	-9.9
			Levofloxacin	-9.0
Anticancer	Tubulin	1SA0	OBA	-8.5
			Colchicine	-8.0
	CDK2	1FIN	OBA	-7.9
			Roscovitine	-6.4

The docking results indicate that the novel compound OBA exhibits strong binding affinities toward multiple target proteins, suggesting promising therapeutic potential. For antibacterial activity, the novel compound OBA binds to Topoisomerase IV with a predicted binding energy of -9.9 kcal/mol, which is slightly stronger than the reference ligand Levofloxacin (-9.0 kcal/mol), indicating that the novel compound OBA could effectively inhibit this critical enzyme involved in DNA replication. In terms of anticancer activity, the novel compound OBA demonstrates notable interactions with both Tubulin and CDK2. For Tubulin, the novel compound OBA shows a binding energy of -8.5 kcal/mol, outperforming Colchicine (-8.0 kcal/mol), which suggests potential disruption of microtubule dynamics. Similarly, OBA binds to CDK2 with an energy of -7.9 kcal/mol, significantly stronger than the reference ligand Roscovitine (-6.4 kcal/mol), implying possible inhibition of cell cycle progression. Overall, the novel compound OBA consistently shows stronger or comparable binding compared to standard reference ligands across all tested targets, highlighting its potential as a multi-target compound with both antibacterial and anticancer activities. These results provide a strong basis for further experimental validation to confirm its efficacy and selectivity (Figs. 7-9).

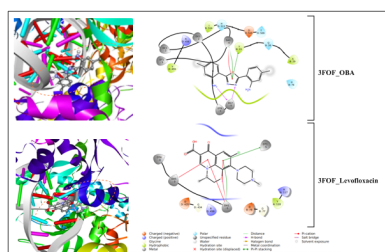


Fig. 7. 2D and 3D interaction profiles of the novel compound OBA and reference ligand Levofloxacin with the active sites of Topoisomerase IV (PDB ID: 3FOF) for antibacterial activity.

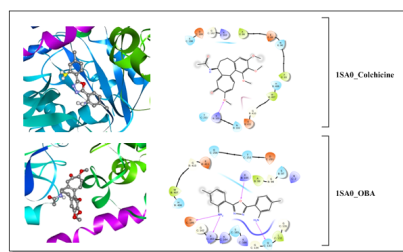


Fig. 8. 2D and 3D Interaction Profiles of the novel compound OBA and Reference Ligand Colchicine with the Active Site of Tubulin (PDB ID: 1SA0) for anticancer activity.

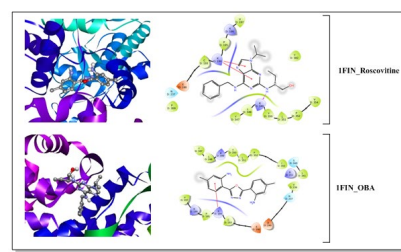


Fig. 9. 2D and 3D Interaction Profiles of the novel compound OBA and Reference Ligand Roscovitine with the Active Site of CDK2 (PDB ID: 1FIN) for anticancer activity.

3.6 Monte Carlo simulation, and MD results

To complement the quantum chemical and docking analyses, Monte Carlo (MC) and Molecular Dynamics (MD) simulations were carried out to explore the adsorption behavior of the novel compound OBA on the Fe(110) surface. These simulations provide atomistic insight into the interaction strength, adsorption stability, and surface coverage of the inhibitor. The combined results offer a detailed understanding of the corrosion inhibition mechanism of the novel compound OBA under dynamic conditions.

Table 5. Monte Carlo simulation results

Structures	Total energy	Adsorption energy	Rigid adsorption energy	Deformation energy	OBA: dEad/dNi	H ₂ O : dEad/dNi	H ₃ O ⁺ & Cl ⁻ : dEad/dNi
Fe(110)	-3.41E+003	-3.42E+003	-3.57E+003	152.01	-128.66	-17.62	-8.51

The Monte Carlo simulation results (**Table 5** and **Fig. 10**) provide detailed insights into the adsorption behavior of the novel compound OBA on the Fe(110) surface. The total energy of the system is -3.41×10^3 kcal/mol, indicating overall thermodynamic stability. The adsorption energy is highly negative at -3.42×10^3 kcal/mol, suggesting a strong exothermic interaction between the novel compound OBA and the metallic surface, indicative of a highly favorable adsorption process. The rigid adsorption energy of -3.57×10^3 kcal/mol represents the adsorption contribution without structural relaxation, highlighting the role of non-covalent interactions such as van der Waals forces and electrostatic effects. The deformation energy of 152.01 kcal/mol reflects the structural adjustments of the molecule and the surface during adsorption, suggesting partial chemisorption where the novel compound OBA adapts its conformation to form stable interactions. Furthermore, the energy per adsorption site values for the novel compound OBA (-128.66 kcal/mol), water (-17.62 kcal/mol), and H₃O⁺/Cl⁻ ions (-8.51 kcal/mol) demonstrate that the novel compound OBA contributes most significantly to the total adsorption energy, confirming its strong affinity for the Fe(110) surface and its potential effectiveness as a surface modifier under aqueous or ionic conditions.

Table 6. Molecular Dynamic results

System	Energy (kcal/mol)
OBA	11.049
Fe + 200 H ₂ O + 8 H ₃ O ⁺ + 8 Cl ⁻	-68883.283
Complex (OBA + Fe + 200 H ₂ O + 8 H ₃ O ⁺ + 8 Cl ⁻)	-68719.100
Interaction energy E_{int}	45.756
Binding energy E_{bind}	-45.756

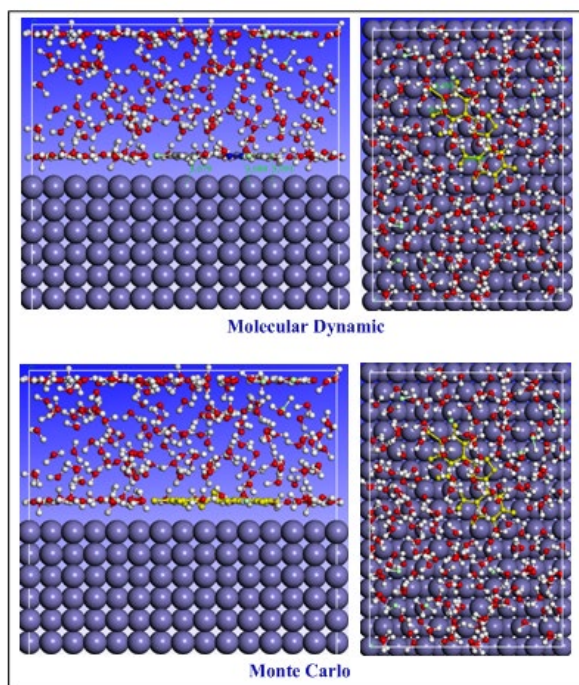


Fig. 10. Across-Plane and Surface Visualization of the novel compound OBA Adsorption on Fe(110) from Molecular Dynamics and Monte Carlo Simulations.

The Molecular Dynamics (MD) simulation results (**Table 6** and **Fig. 10**) provide detailed insights into the thermodynamic and structural behavior of the novel compound OBA interacting with the Fe(110) surface under dynamic

conditions. The total energy of the isolated the novel compound OBA molecule is 11.049 kcal/mol, while the Fe (110) surface solvated with 200 water molecules and 8 H₃O⁺/8 Cl⁻ ions has a total energy of -68883.283 kcal/mol. The combined system, including the novel compound OBA adsorbed on the solvated Fe (110) surface, has a total energy of -68719.100 kcal/mol. The calculated interaction energy of 45.756 kcal/mol indicates the net energy contribution arising from the interaction between the novel compound OBA and the metal-solvent environment, while the corresponding binding energy of -45.756 kcal/mol reflects a favorable and spontaneous adsorption process. These results suggest that the novel compound OBA forms stable interactions with the Fe (110) surface in the presence of water and ionic species, maintaining a planar conformation that maximizes surface contact. The MD simulations highlight the influence of the solvent environment and dynamic fluctuations, showing that the novel compound OBA adsorption remains energetically favorable and structurally stable, which supports its potential effectiveness as a surface modifier or corrosion inhibitor under realistic aqueous conditions.

4. Conclusion

This study confirms the structure of a novel 1,3,4-oxadiazole derivative, the novel compound 6,6'-(1,3,4-Oxadiazole-2,5-diyl)bis(3-chloroaniline), by ¹H NMR, ¹³C NMR, mass spectrometry and FTIR-ATR infrared spectroscopy. DFT calculations provided insight into its electronic structure and reactive sites, while molecular docking revealed strong interactions with antibacterial and anticancer targets. Monte Carlo and Molecular Dynamics simulations demonstrated stable adsorption on the Fe (110) surface, highlighting its potential as an efficient corrosion inhibitor. These combined experimental and theoretical results confirm the multifunctional character of the compound and its applicability in both medicinal and material chemistry.

Funding

The authors declare that no funds, grants, or other supports were received during the preparation of this manuscript.

Acknowledgements

The authors are grateful to for the research assistance from Bioorganic Chemistry Team, Faculty of Sciences, Chouaib Doukkali University, B.P. 20, 24000 El Jadida, Morocco and Molecular Modeling and Spectroscopy Research Team, Faculty of Science, ChouaibDoukkali University, P.O. Box 20, 24000 El Jadida, Morocco.

References

1. Salahuddin M. A., Yar M. S., Mazumder R., Chakraborty G. S., Ahsan M. J., and Rahman M. U. (2017) Updates on synthesis and biological activities of 1, 3, 4-oxadiazole: A review. *Synth. Commun.*, 47 (20) 1805-1847.
2. Al-Mulla A. (2017) A review: biological importance of heterocyclic compounds. *DPC.*, 9 (13) 141-147.
3. Salassa G., and Terenzi A. (2019) Metal complexes of oxadiazole ligands: An overview. *Int. J. Mol. Sci.*, 20 (14) 3483-3500.
4. Kaur R., and Kaur P. (2018) Synthesis and pharmacological activities of 1, 3, 4-oxadiazole derivatives: A review. *Eur. J. Biomed. Inform.*, 5 (6) 865-877.
5. Omar A. (2020) Review article; anticancer activities of some fused heterocyclic moieties containing nitrogen and/or sulfur heteroatoms. *Al-Azhar J. Pharm. Sci.*, 62 (2) 39-54.
6. Atif A., El Alami A., and Ait Sir H. (2025) Minireview of Synthesis Process of 1,3,4-Thiadiazole Derivatives. *Chem. Afr.*, 8 (7) 2663-2686
7. Atif A., and Ait Sir H. (2025) Progress in the Synthesis of Tetrazoles. A Brief Review. *Org. Prep. Proced. Int.*, 57 (6) 497-512
8. Atif A., and Ait Sir H. (2025) Synthetic Approaches for Oxazole Derivatives: A Review. *J. Heterocycl. Chem.*, 6 (2) 1808-1833.
9. Shiri P. (2020) An overview on the copper-promoted synthesis of five-membered heterocyclic systems. *Appl. Organomet. Chem.*, 34 (5) e5600-e5617.
10. Baranwal J., Kushwaha S., Singh S., and Jyoti A. (2023) A review on the synthesis and pharmacological activity of heterocyclic compounds. *Curr. Phys. Chem.*, 13 (1) 2-19.
11. Lata S., Choudhary L., Bharwal A., Pandit A., and Abbot V. (2025). A Comprehensive Review: Synthesis and Pharmacological Activities of 1, 3, 4-Oxadiazole Hybrid Scaffolds. *Med. Chem.*, 21 (10) 1051-1071
12. Biernacki K., Daško M., Ciupak O., Kubiński K., Rachon J., and Demkowicz S. (2020) Novel 1, 2, 4-oxadiazole derivatives in drug discovery. *Pharma.*, 13 (6) 111-156.
13. El-Masry R. M., Kadry H. H., Taher A. T., and Abou-Seri S. M. (2022) Comparative study of the synthetic approaches and biological activities of the bioisosteres of 1, 3, 4-oxadiazoles and 1, 3, 4-thiadiazoles over the past decade. *Mol.*, 27 (9) 2709-2729.
14. Ali A., Hasan P., Irfan M., Uddin A., Khan A., Saraswat J., Maguire R., Kavanagh K., Patel R., Joshi M. C., Azam A., Mohsin M., Mohd Q., Haque R., and Abid M. (2021) Development of oxadiazole-sulfonamide-based compounds as potential antibacterial agents. *ACS omega*, 6 (42) 27798-27813.

15. Xie Y. P., Sangaraiah N., Meng J. P., and Zhou C. H. (2022) Unique carbazole-oxadiazole derivatives as new potential antibiotics for combating Gram-positive and-negative bacteria. *J. Med. Chem.*, 65 (8) 6171-6190.
16. Omidi B., and SarveAhrabi Y. (2021) In vitro and in silico evaluation of biological properties of some 1, 3, 4-oxadiazole derivatives against *Streptococcus mutans* and their interaction with Gbp-C by molecular docking. *Avicenna J. Dent. Res.*, 13 (4) 142-147.
17. Wan M. C., Qin W., Lei C., Li Q. H., Meng M., Fang M., Song W., Chen J., Tay F., and Niu L. N., (2021) Biomaterials from the sea: Future building blocks for biomedical applications. *Bioact. Mater.*, 6 (12) 4255-4285.
18. Kiddle J. J. (1995) Quebrachitol: a versatile building block in the construction of naturally occurring bioactive materials. *Chem. Rev.*, 95 (6) 2189-2202.
19. Narayanankutty A., Famurewa A. C., and Oprea E. (2024) Natural bioactive compounds and human health. *Mol.*, 29 (14) 3372-3379.
20. Singh R., and Vince R. (2012) 2-Azabicyclo [2.2. 1] hept-5-en-3-one: chemical profile of a versatile synthetic building block and its impact on the development of therapeutics. *Chem. Rev.*, 112 (8) 4642-4686.
21. Chakraborty T. K., Ghosh S., and Jayaprakash S. (2002) Sugar amino acids and their uses in designing bioactive molecules. *Curr. Med. Chem.*, 9 (4) 421-435.
22. Narayanan B., Redfern P. C., Assary R. S., Curtiss L. A. (2019) Accurate quantum chemical energies for 133000 organic molecules. *Chem. Sci.*, 10 (31) 7449-7455.
23. Deglmann P., Schäfer A., and Lennartz C. (2015) Application of quantum calculations in the chemical industry—an overview. *Int. J. Quantum Chem.*, 115 (3) 107-136.
24. Falowska A., Zabkowska M., Sambora K., Kula K., Lapczuk A., and Jasinski, R. (2025) Application of DFT models for the prediction of geometries and energies of the transition states in [4+2]-p-electron cycloadditions. *Curr. Chem. Lett.*, 15 (1) 169-174
25. Ghalibafi A., and Pakravan P. (2025) A systematic theoretical approach on using some heteroatom-decorated BC10N nanosheets for drug delivery of carmustine. *Chem. Heterocycl. Compd.*, 61 (7) 1-8.
26. Messaadia S., Chafaa F., Bouabbaci H., and Nacereddine A. K. (2025) Computational mechanistic study of the Diels–Alder reaction between the N-substituted exocyclic oxazolidin-2-one diene and symmetric bis-chalcone. *Chem. Heterocycl. Compd.*, 61 (7) 341-348.
27. El Haib A., Hakmaoui Y., Asserne F., Rabbah B., Raji H., Chennani A., Benharref A., and Zeroual, A. (2025) Theoretical study of the molecular mechanism and regioselectivity of the (3+ 2) cycloaddition reaction between benzonitrile oxide and 2, 4-dimethyl-2H-1, 2, 3-triazole and molecular docking studies of the obtained cycloadducts. *Chem. Heterocycl. Compd.*, 61 (7) 355-365.
28. Ferreira L. G., Dos Santos R. N., Oliva G., and Andricopulo A. D. (2015) Molecular docking and structure-based drug design strategies. *Mol.*, 20 (7) 13384-13421.
29. Atif A., Ameer S., Bendaoud A., Hsissou R., Jebbari S., Ait Sir H., and Salah M. (2025) Comprehensive evaluation of a benzimidazole-1,3,4-oxadiazole derivative for corrosion protection of C38 steel in HCl: Experimental, molecular dynamics, monte carlo, and in silico pharmacokinetic approaches. *Curr. Chem. Lett.*, 14 (4) 777-792
30. Atif A., Ameer S., and Ait Sir H. (2025) Synthesis, characterization and in silico evaluation of 2,5-bis(2-(trifluoromethyl)-1Hbenzimidazol-5-yl)-1,3,4-oxadiazole: Reactivity, ADME/toxicity, and docking against therapeutic targets. *Curr. Chem. Lett.*, 14 (4) 793-804
31. Fuster F., Sevin A., and Silvi B. (2000) Topological analysis of the electron localization function (ELF) applied to the electrophilic aromatic substitution. *J. Phys. Chem. A*, 104 (4) 852-858.
32. Spivak M., Stone J. E., Ribeiro J., Saam J., Freddolino L., Bernardi R. C., and Tajkhorshid E. (2023) VMD as a platform for interactive small molecule preparation and visualization in quantum and classical simulations. *J. Chem. Inf. Model.*, 63 (15) 4664-4678.
33. Pires D. E. V., Blundell T.L., and Ascher D. B. (2015) PkCSM: Predicting Small-Molecule Pharmacokinetic Properties Using Graph-Based Signatures. *J. Med. Chem.*, 58 (9) 4066-4072
34. Trott O., and Olson A. J. (2010) AutoDock Vina: improving the speed and accuracy of docking with a new scoring function, efficient optimization, and multithreading. *J. Comput. Chem.*, 31 (2) 455-461.
35. Doudna J. A., and Richmond T. J. (2001) Protein–nucleic acid interactions. *Curr. Opin. Struct. Biol.*, 11 (1) 11-13.
36. Kim S., Chen J., Cheng T., Gindulyte A., He J., He S., Li Q., Shoemaker B. A., Thiessen P. A., Yu B., Zaslavsky L., Zhang J., and Bolton E. E. (2021) PubChem in 2021: new data content and improved web interfaces. *Nucleic Acids Res.*, 49 (D1) D1388-D1395.
37. Atif A., Ameer S., Ait Sir H. (2025) Synthesis, Characterization, and Computational Investigation of 2,5-Bis(2-Methyl-1H-benzimidazol-5-yl)-1,3,4-oxadiazole: Quantum Chemical Analysis, ADME Prediction, Molecular Docking, and MD-Based Corrosion Study for Photonic and Therapeutic Applications”. *Curr. Chem. Lett.*, 15 (1) 133-146
38. Atif A., El Alami A., Youssoufi F., Jebbari S., Ait Sir H. (2025) Review of synthesis process of 1,3,4-oxadiazole analogs. *Curr. Chem. Lett.*, 14 (2) 339–364
39. Atif A., Marghich M., Nabil N., El Alami A., Daoudi N., Harit T., Youssoufi F., Salah M., Bitar A., and Ait Sir, H. (2025) Design, synthesis, and antidiabetic evaluation of novel 1,3-di(1,3,4-oxadiazol-2-yl)benzene derivatives as potent pancreatic α -amylase inhibitors: In vitro and in silico approaches. *Curr. Chem. Lett.*, 15 (1) 175–192
40. Atif A., Zahm S., Jebbari S., El Alami A., Youssoufi F., Ait Sir H., Kerraj S., and Salah M. (2023) Synthesis, Admet, Docking and Molecular Dynamics of New Molecules Derivatives from 1,3,4-Oxadiazole and 1,3,4-Bisoxadiazole: New Compounds Against HIV. *Eur. Chem. Bull.*, 12 (12) 4139-4156

41. Atif A., Ahmed B., Ait Sir H., Mohammed S., and Abdellah, Z. (2026) Synthesis, characterization and computational investigation of 5-chloro-2-(5-(2-methyl-1H-benzimidazol-5-yl)-1,3,4-oxadiazol-2-yl)aniline: DFT, parr indices, ADMET, molecular docking and molecular dynamics. *Curr. Chem. Lett.*, 15 (1) 101-116



© 2026 by the authors; licensee Growing Science, Canada. This is an open access article distributed under the terms and conditions of the Creative Commons Attribution (CC-BY) license (<http://creativecommons.org/licenses/by/4.0/>).